Journal of Porous Media, 2(1), 87–106 (1999)

Magnetohydrodynamic Mixed Convection from a Rotating Cone Embedded in a Porous Medium with Heat Generation

Ali J. Chamkha

Department of Mechanical and Industrial Engineering,
Kuwait University, P.O. Box 5969, Safat 13060, Kuwait

ABSTRACT

A similarity transformation is employed to convert the partial differential equations governing steady, laminar, hydromagnetic, mixed convection from a rotating non-isothermal and permeable cone embedded in a uniform non-Darcian porous medium into ordinary ones. The coupled nonlinear equations are solved numerically by an iterative implicit finite-difference method. Comparisons with previously published work are performed and found to be in excellent agreement. Graphical results are presented to show the influence of the possible presence of wall mass transfer, heat generation effects, magnetic field, and porous media.

Received August 25, 1997; Accepted December 1, 1997

INTRODUCTION

This article deals with the steady, laminar, mixed convection flow of a viscous, Newtonian, electrically conducting and heat-generating/absorbing fluid induced by a nonisothermal rotating cone embedded in a porous medium. This flow and heat transfer situation is of considerable interest to the technical field owing to its frequent occurrence in many industrial, technological, and geothermal applications such as atmospheric and oceanic circulations, filtration, nuclear reactors, power transformers, vortex chambers (Kumari et al., 1993), and shielding of a rotating body from excessive heating (Kumar et al., 1988). The geothermal gases are electrically conducting and are affected by the presence of a magnetic field. The same is found regarding the cooling of nuclear reactors (see Aldoss et al., 1995). Such a problem may also have relevance in areas of geophysics and astrophysics such as hydromagnetic flow and heat transfer in the earth's liquid core, existence of geomagnetic field, rotation of stars, and others (Takhar et al., 1987). It is worth mentioning that magnetohydrodynamic flow and heat transfer in porous and nonporous geometries have been considered by many investigators (see, for instance, Sparrow and Cess, 1961; Riley, 1964; Raptis and Kafoussias, 1982; Raptis and Singh, 1983; Raptis, 1986; Hossain, 1992; Kafoussias, 1992; Takhar and Ram, 1994; Aldoss et al., 1995; Chamkha, 1996). Other related works dealing with heat generation or absorption effects can be found in the articles by Moalem (1976), Vajravelu and Nayfeh (1992), Chamkha (1996, 1997), and the references therein.

Early work, on flow in porous media used the Darcy law, which is applicable to slow flows and does not account for inertial and boundary effects (termed as non-Darcy effects) that become important where the flow velocity is relatively high and in the presence of a boundary. The condition of high velocity is realized when the pressure drop across the porous medium is a quadratic function of the velocity. Vafai and Tien (1981) reported a detailed discussion on these non-Darcian effects. Mixed convection flows along vertical plates and other geometries embedded in porous media with Darcian and non-Darcian effects have been reported by many authors (see, for example, Hsu and Cheng, 1985; Minkowycz et al., 1985; Lai and Kulacki, 1991; Nield, 1991; Hsieh et al., 1993; Aldoss et al., 1994; Chamkha, 1997).

The flow and heat transfer situation resulting from rotating surfaces is thoroughly reviewed by Kreith (1968). The problem of a rotating cone or disk in the absence or presence of a magnetic field has received considerable attention over the years. Tien (1960) considered forced convection flow from a rotating isothermal cone. Hartnett and Deland (1961) studied the effects of Prandtl number on heat transfer from rotating nonisothermal disks and cones. Hering and Grosh (1963) investigated combined convection from a rotating nonnisothermal cone. Oehlbeck and Erian (1979) reported heat transfer results for axisymmetric heat sources at the surface of a rotating disk. Himasekhar and Sarma (1984, 1986a,b) analyzed combined convection for a rotating permeable cone in thermally uniform and stratified environments. Takhar et al. (1987) investigated unsteady boundary-layer flows over a rotating disk with an applied magnetic field. Lin and Lin (1987) proposed a new similarity variable for flow and heat transfer from rotating cones and disks. Wang and Kleinstreuer (1990) considered combined convection from a rotating cone or disk for non-Newtonian fluids. Gorla (1992) reported on the effects of uniform wall suction as the magnetohydrodynamic flow over a rotating disk. Kumari et al. (1993) analyzed the problem of unsteady, hydromagnetic, free-convection flow over a rotating disk. In addition, the problem of mixed convection from a rotating nonisothermal cone was studied by Wang et al. (1994) in terms of nonsimilarity equations. Motivated by all previously mentioned references, it is of interest in the present article to consider hydromagnetic mixed convection from a rotating cone embedded in a porous medium with heat generation/absorption and wall suction or blowing.

GOVERNING EQUATIONS

Consider steady, laminar mixed convection flow of an electrically conducting and heat-generating/absorbing fluid induced by a rotating cone embedded in a uniform fluid-saturated porous medium. The configuration of the rotating cone and the coordinate system are shown in Fig. 1. A uniform magnetic field is applied in the z direction normal to the cone surface. The surface of the cone is maintained at a nonisothermal temperature $T_w(x)$ and is assumed to be permeable so that fluid suction or blowing can be applied. All fluid properties are assumed to be constant except the density variations in the buoyancy force in the x-momentum equation. The magnetic Reynolds number is assumed to be small so that the induced magnetic field can be neglected. In addition, the Hall effect of magnetohydrodynamics and Ohmic heating are neglected and it is assumed that there is no applied electric field and, therefore, no electromagnetic work exists. Furthermore, it is assumed that both the fluid and the porous medium do-

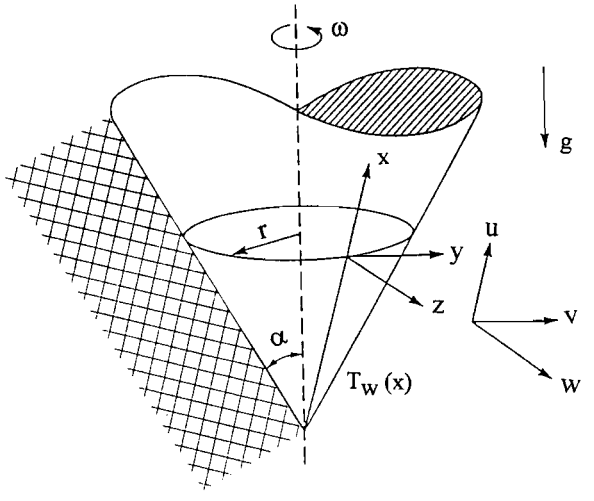

Figure 1. Flow model and coordinate system.

mains are in local thermal equilibrium and that the cone is made of a nonelectrically conducting material. The governing equations for this investigation are based on the balance laws of mass, linear momentum, and energy modified to account for the magnetic field, buoyancy force, Darcian and non-Darcian porous medium effects, heat generation/absorption effects, and the wall mass transfer effects. Under the usual boundary-layer and Boussinesq approximation, these equations can be written as (see Hering and Grosh, 1963 and Aldoss et al., 1995)

$$\frac{\partial u}{\partial x}+\frac{\partial w}{\partial z}+\frac{u}{x}=0 \tag{1}$$

$$\rho\left(u\frac{\partial u}{\partial x}+w\frac{\partial u}{\partial z}-\frac{v^2}{x}\right)=-\frac{dp}{dx}+\mu\frac{\partial^2 u}{\partial x^2}-\sigma B_o^2 u-\frac{\mu}{K}u - Cu^2-\rho g\cos\alpha \tag{2}$$

$$\rho\left(u\frac{\partial v}{\partial x}+w\frac{\partial v}{\partial z}+\frac{uv}{x}\right)=\mu\frac{\partial^2 v}{\partial z^2}-\frac{\mu}{K}v-Cv^2-\sigma B_o^2 v \tag{3}$$

$$\rho c_p\left(u\frac{\partial T}{\partial x}+w\frac{\partial T}{\partial z}\right)=k_e\frac{\partial^2 T}{\partial z^2}+Q_o(T-T_\infty) \tag{4}$$

where x, y, and z are the tangential, circumferential, and normal distances, respectively. u, v, w, p, and T are the fluid's velocity components in the x, y, and z directions; pressure; and temperature, respectively. ρ, μ, and c_p are the fluid's density, dynamic viscosity, and specific heat at constant pressure, respectively. σ, B_o, g, and α are the fluid's electrical conductivity and magnetic induction, the gravitational acceleration, and the cone apex half angle, respectively. K, C, k_e, and Q_o are the porous medium permeability, inertia coefficient, effective thermal conductivity, and the heat generation/absorption coefficient, respectively. A subscript ∞ denotes a property at the ambient condition. It should be noted that aiding flows are designated as those flows for which the buoyancy force has a positive component in the direction of increasing distance from the cone apex. On the other hand, opposing flows correspond to the situation for which the buoyancy force has a positive component in the opposite direction. These flows are reflected by a sign change in the term $-\rho g\cos\alpha$ of Eq. (2) (see Hering and Grosh, 1963). Furthermore, it should be mentioned that positive values of Q_o indicate heat generation (source) while negative values of Q_o correspond to heat absorption conditions (sink). Also, the heating (or cooling) source (or sink) appearing in the last term of Eq. (4) is assumed to vary linearly with temperature as done by Vajravelu and Nayfeh (1992), as this is required to obtain a similarity solution.

Evaluation of Eq. (2) at the ambient conditions yields the following expression for the hydrostatic pressure gradient:

$$\frac{dp}{dx}=-\rho_\infty g\cos\alpha \tag{5}$$

Substituting Eq. (5) into Eq. (2), combining with the buoyancy term, and introducing the coefficient of thermal expansion β produce the following approximate form of Eq. (2):

$$\rho\left(u\frac{\partial u}{\partial x}+w\frac{\partial u}{\partial z}-\frac{v^2}{x}\right)=\mu\frac{\partial^2 u}{\partial z^2}+\rho g\beta(T-T_\infty)\cos\alpha - \sigma B_o^2 u-\frac{\mu}{K}u-Cu^2 \tag{6}$$

It should be reminded that the first and last terms on the right-hand side of Eq. (6) represent the x-components of the non-Darcian boundary and inertia effects (see Vafai and Tien, 1981). Also, the term $\sigma B_o^2 u$ on the right-hand side of the same equation signifies the x-component electromagnetic body force.

The physics of the problem under consideration suggests the following boundary conditions:

$$\begin{aligned} &z=0:\ u=0,\ v=r\omega,\ w=-w_o,\ T=T_w(x)\\ &z=\infty:\ u=0,\ v=0,\ T=T_\infty \end{aligned} \tag{7}$$

where r is the cone radius, ω is the angular velocity of rotation, and w_0 (a constant) is the normal velocity at the wall, respectively. It should be mentioned that positive

values of w_0 indicate fluid suction at the cone surface while negative values of w_0 correspond to the case of injection at the wall.

It has been demonstrated by previous investigators (see Tien, 1960 and Merk and Prins, 1953) that similarity transformations exist for both free and forced convection from isothermal cone. Following Tien (1960), Hering and Grosh (1963), and later Himasekhar and Sarma (1986b), the following similarity transformation is introduced:

$$\eta = (\omega \sin\alpha/\nu)^{1/2} z$$
$$u = x\omega \sin\alpha F(\eta), \quad v = x\omega \sin\alpha G(\eta) \tag{8}$$
$$w = (\nu\omega \sin\alpha)^{1/2} H(\eta), \; T - T_\infty = (T_w(x) - T_\infty)\theta(\eta)$$

where $\nu(=\mu/\rho)$ is the kinematic viscosity of the fluid. It should be noted that with the use of Eq. (8) the case of nonrotating cone ($\omega = 0$) will be excluded from the present work. In addition, it should be understood that all the results to be reported in the next section are not valid near the leading edge ($x = 0$) due to the presence of a singularity there.

It can easily be shown, as done by Hering and Grosh (1963), that a similarity solution exists if the wall temperature distribution is a linear function of x. Substituting Eq. (8) into Eq. (1), (3), (4), and (6) with $T_w(x) - T_\infty = (T_L - T_\infty)\, x/L$ [L being the cone slant height and T_L being the cone surface temperature at the base ($x = L$)] yields

$$H' + 2F = 0 \tag{9}$$

$$F'' - HF' - (1 + \Gamma_x)F^2 - (M^2 + D_a^{-1})F + G^2 + \frac{Gr}{Re^2}\theta = 0 \tag{10}$$

$$G'' - HG' - 2FG - (M^2 + D_a^{-1})G - \Gamma_x G^2 = 0 \tag{11}$$

$$\theta'' - Pr(H\theta' + F\theta - \phi\theta) = 0 \tag{12}$$

where a prime denotes ordinary differentiation with respect to η. $M^2 = \sigma B_o^2/(\rho\omega \sin\alpha)$, $D_a^{-1} = \nu/(K\omega \sin\alpha)$, $\Gamma_x = Cx/\rho$, $Gr = g\beta(T_w(x) - T_\infty)x^3 \cos\alpha/\nu^2$, $Re = \omega x^2 \sin\alpha/\nu$, $Pr = \mu c_p/k_e$, and $\phi = Q_o/(\rho c_p \omega \sin\alpha)$ are the square of the Hartmann number, the inverse Darcy number, the dimensionless porous medium inertia coefficient, the local Grashof number, the local Reynolds number, the Prandtl number, and the dimensionless heat generation/absorption coefficient, respectively. It is important to mention here that the existence of similar equations also requires that the inertia coefficient $C = C(x)$ is inversely proportional to x. Otherwise, Eqs. (9) through (12) will be locally similar equations.

The transformed form of the boundary conditions (7) for this problem become

$$\begin{aligned} &\eta = 0: \; H' = 0, \; G = 1.0, \; H = -h_0, \; \theta = 1.0 \\ &\eta = \infty: \; H' = 0, \; G = 1.0, \; \theta = 0 \end{aligned} \tag{13}$$

where $h_0 = w_0/(\nu\omega \sin\alpha)^{1/2}$ is the dimensionless wall mass transfer coefficient.

Important physical parameters for this flow and heat transfer situation are the local friction factor, moment coefficient, and the local heat transfer rate. These quantities are defined in dimensionless form, respectively, as

$$C_{fy} = \frac{\tau_y}{\left(\frac{1}{2}\rho(x\omega \cos\alpha)^2\right)} = \frac{2G'(0)}{\sqrt{Re}}, \quad \tau_y = \mu\left(\frac{\partial v}{\partial z}\right)_{z=0} \tag{14}$$

$$C_M = \frac{M^*}{\frac{1}{2}\rho(L\omega \cos\alpha)^2 r_0^3} = \frac{-\pi G'(0)}{\sqrt{Re} \sin\alpha},$$

$$M^* = -\int_0^L r\tau_y 2\pi r \, dx \tag{15}$$

$$N_q = \frac{qx}{k_e(T_w(x) - T_\infty)} = -Re^{1/2}\theta'(0), \; q = -k_e\left(\frac{\partial T}{\partial z}\right)_{z=0} \tag{16}$$

where τ_y is the shear stress, M^* is the shaft moment torque required to overcome the shear of the rotating cone, q is the dimensional heat transfer rate per unit area, and r_o is the cone radius at the base ($x = L$).

NUMERICAL SOLUTION

The boundary-value problem represented by the nonlinear, coupled ordinary differential Eqs. (9) through (12) subject to the boundary conditions (13) possesses no closed-form solution. Therefore, a numerical solution is required to solve the present problem. The implicit finite-difference method discussed by Blottner (1970) have proven to be successful for the numerical solution of this type of equations. This method is similar to the Keller's box method discussed by Cebeci and Bradshaw (1977). For this reason, it is adopted herein for the solution of this problem.

Equations (10) through (12) are discretized using three-point central difference quotients while Eq. (9) is discretized by the trapezoidal rule. A nonuniform mesh distribution is used to accommodate steep velocity and temperature gradients in the immediate vicinity of the cone surface. The computational domain was divided into 195 nodes and the initial step size $\Delta\eta_1 = 0.001$ and the growth factor $K^* = 1.03$ were employed such that $\Delta\eta_{i+1} = K^* \Delta\eta_i$. These values give a location of the boundary-layer edge $\eta_\infty \cong 10$ and were arrived at after many numerical experimentations were performed to assess grid independ-

ence. With the above mentioned discretization procedure, linear tridiagonal algebraic equations result. These equations are solved by the Thomas Algorithm (see Blottner, 1970) with iteration being employed to deal with the nonlinearities of the governing equations. A convergence criterion based on the relative difference between the current and the previous iterations is employed. When this difference reached 10^{-5}, the solution was assumed converged and the iteration procedure was terminated.

To check the accuracy of the numerical method, a comparison of the present results for $G'(0)$ and $\theta'(0)$ with those reported earlier by Hering and Grosh (1963) for air ($Pr = 0.7$) and in the absence of all of the magnetic, heat generation, wall suction, and the porous medium effects is performed. The results of this comparison are shown in Table 1. As seen from this table, excellent agreement between the results is obtained for various levels of buoyancy effects. This comparison lends confidence to the numerical results to be reported subsequently.

RESULTS AND DISCUSSION

Figures 2 through 5 present representative profiles for the tangential velocity F, circumferential velocity G, normal velocity H, and temperature θ for various values of the Hartmann number M, respectively. In view of its magnetic properties, the parametric values employed to obtain these and all subsequent figures correspond to water ($Pr = 6.7$) flow with heat generation at moderate buoyancy conditions ($Gr/Re^2 = 10$) and without wall mass transfer. Application of a uniform magnetic field in the z direction produces resistive forces in both the x and y directions. These forces act in the direction opposite to that of the flow and tend to reduce the fluid velocity in these directions. However,

Table 1

Comparison of $G'(0)$ *and* $\theta'(0)$ *with those of Hering and Grosh (1963) for various* Gr/Re^2 *values and* $D_a^{-1} = 0$, $h_0 = 0$, $M = 0$, $Pr = 0.7$, $\Gamma_x = 0$, *and* $\theta = 0$

Gr/Re^2	$-G'(0)$ Hering and Grosh (1963)	$-G'(0)$ Present Work	$-\theta'(0)$ Hering and Grosh (1963)	$-\theta'(0)$ Present Work
0	0.61592	0.61703	0.42852	0.43006
0.1	0.65489	0.65608	0.46156	0.46353
1.0	0.85076	0.85204	0.61202	0.61249
10	1.40370	1.40524	1.01730	1.01825
100	2.47380	2.47520	1.79460	1.79622

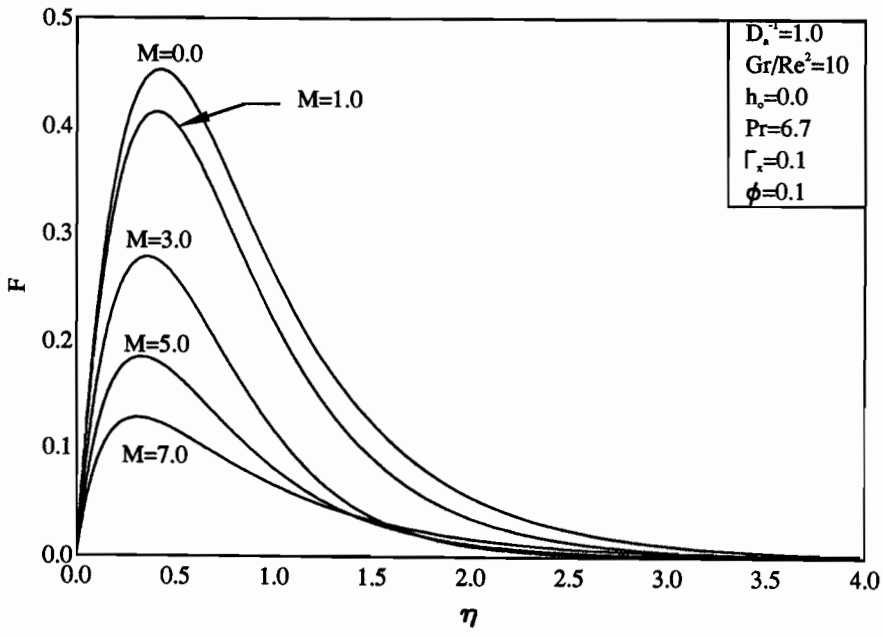

Figure 2. Effects of M on tangential velocity profiles.

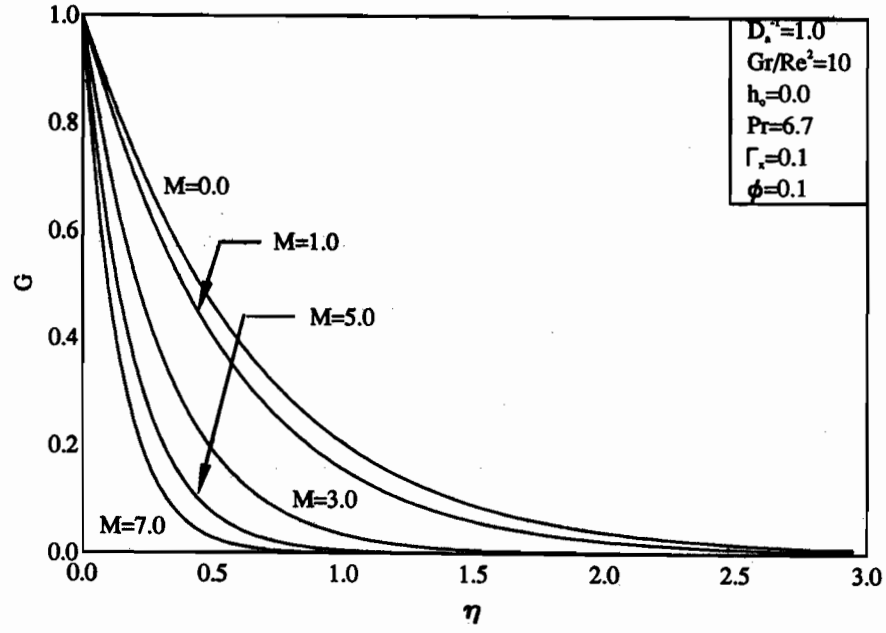

Figure 3. Effects of M on circumferential velocity profiles.

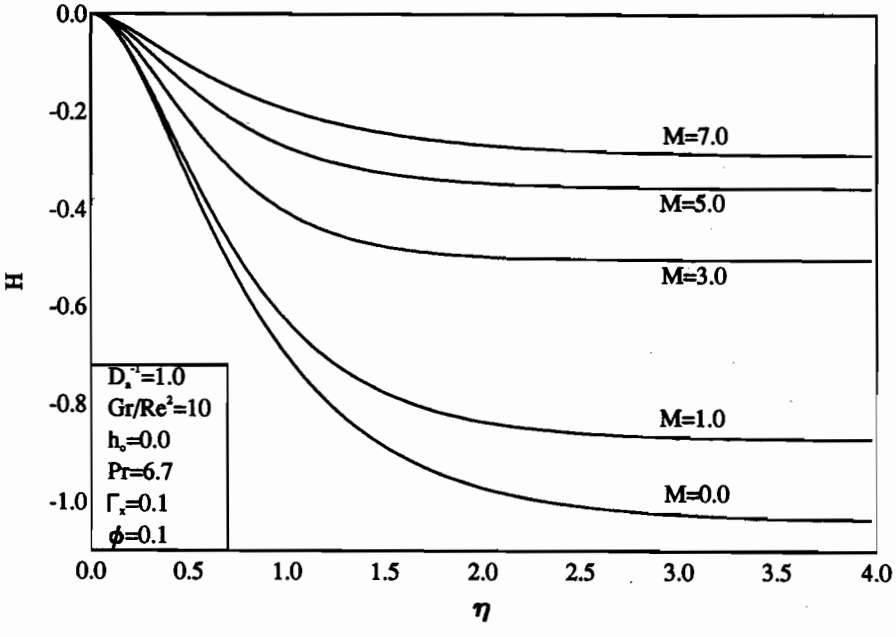

Figure 4. Effects of M on normal velocity profiles.

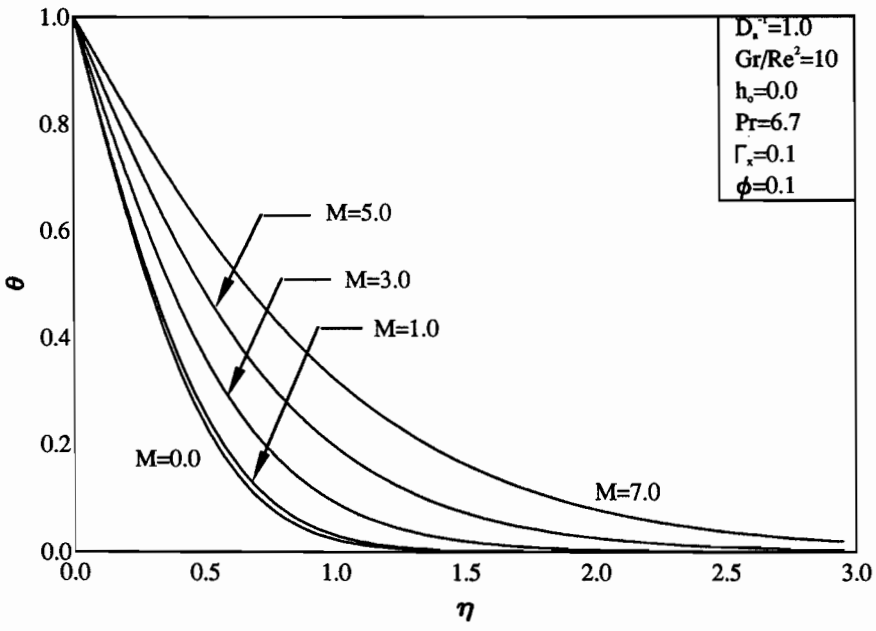

Figure 5. Effects of M on temperature profiles.

both the fluid velocity component in the z direction (normal velocity) and the fluid temperature have the tendency to increase, due to the coupling between the flow and thermal problems, as a result of the presence of the magnetic field. All of these behaviors are clearly depicted by the decreases in F and G and the increases in H and θ shown in Figs. 2 through 5, respectively.

Figures 6 through 9 show the variations in F, G, H, and θ due to the changes in the inverse Darcy number D_a^{-1}, respectively. It is a known fact that the presence of a porous medium represents additional resistance to the flow. This flow resistance has the same effect as that produced by the application of a magnetic field. This is evident from Figs. 6 through 9. It should be mentioned herein that when $D_a^{-1} = 0$, the porous medium inertia coefficient Γ_x is set to zero as well to illustrate the case of a clear (nonporous) domain.

Figures 10 through 13 illustrate the influence of the buoyancy forces on the velocity (F, G, H) and temperature (θ) fields in the boundary layer adjacent to the rotating cone for different values of the buoyancy to viscous forces ratio Gr/Re^2, respectively. Increases in the values of Gr/Re^2 have the tendency to reduce the boundary-layer thickness and increase the fluid mass flow in the neighborhood of the cone. The combination of these two effects produces a rapid increase in the fluid tangential velocity F. Owing to the increase of mass flow of ambient fluid into the boundary layer, the rotational or circumferential (G) and normal (H) velocity components reduce more quickly. Furthermore, the increased flow of ambient fluid in the neighborhood of the cone causes the temperature and the thermal boundary-layer thickness to decrease more rapidly as the buoyancy effect increases. These facts are depicted in the increases in F and decreases in G, H, and θ as the ratio Gr/Re^2 increases shown in Figs. 10 through 13, respectively.

The effects of the fluid Prandtl number Pr and the heat generation/absorption coefficient ϕ on the tangential velocity and temperature distributions are given in Figs. 14 through 17, respectively. As expected, it is observed from these figures that as Pr increases, both the velocity and thermal boundary layer thicknesses decrease, causing reduced temperature and mass flow of ambient fluid in the boundary layer. On the other hand, increasing the heat generation/absorption coefficient produces the opposite effect, namely, an increase in both F and θ. It is also observed from Figs. 16 and 17 that the increases in both F and θ as a result of increasing ϕ occur with no significant changes in the velocity and thermal boundary-layer thicknesses.

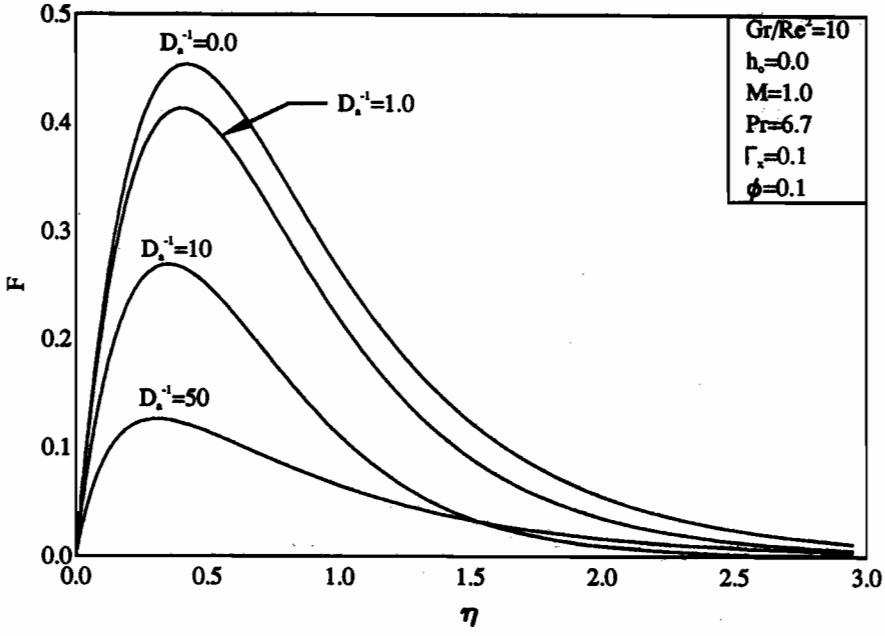

Figure 6. Effects of D_a^{-1} on tangential velocity profiles.

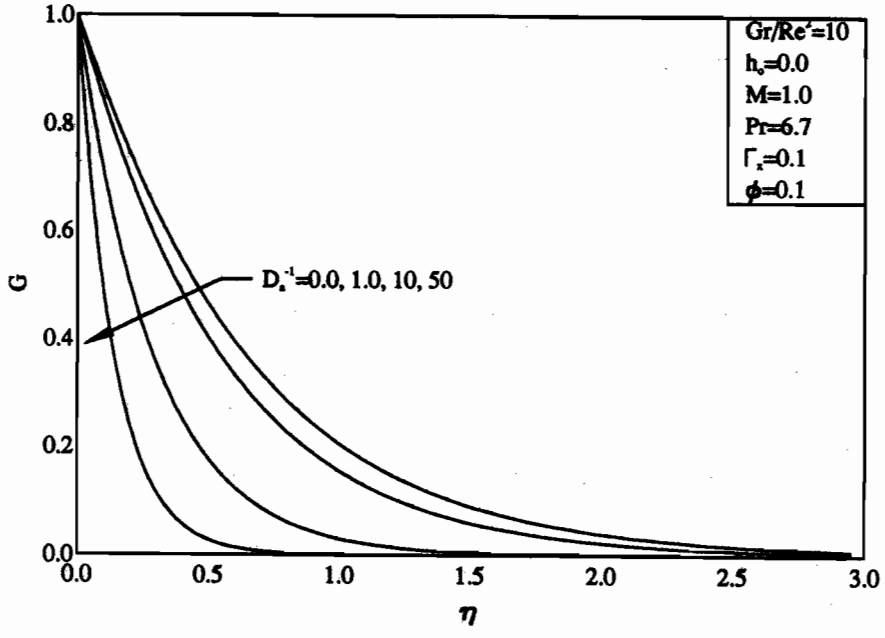

Figure 7. Effects of D_a^{-1} on circumferential velocity profiles.

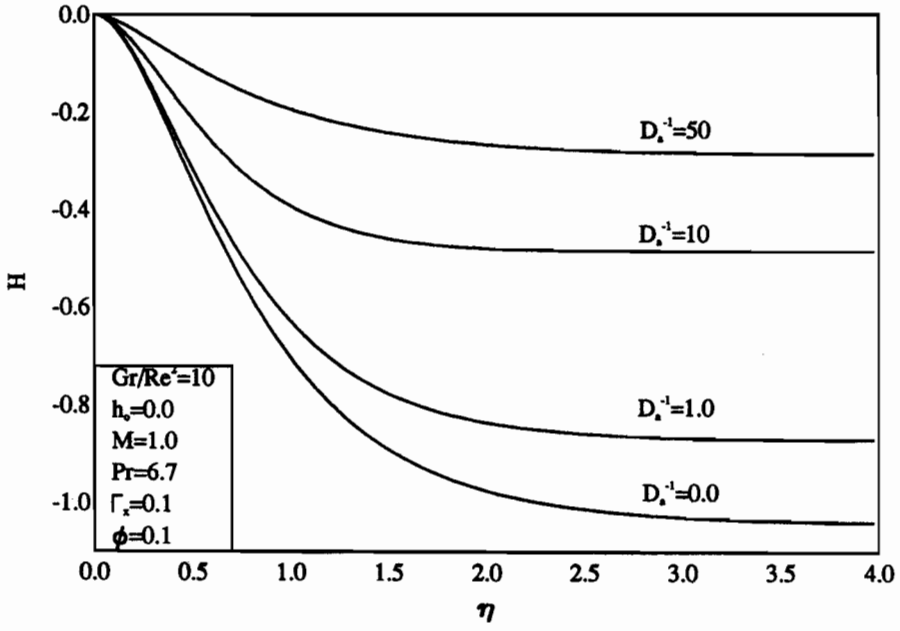

Figure 8. Effects of D_a^{-1} on normal velocity profiles.

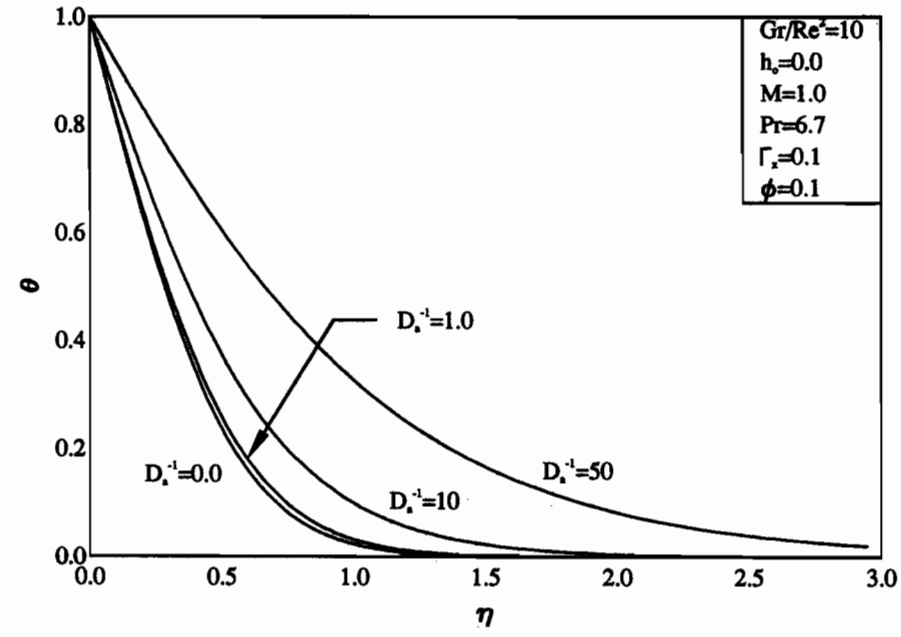

Figure 9. Effects of D_a^{-1} on temperature profiles.

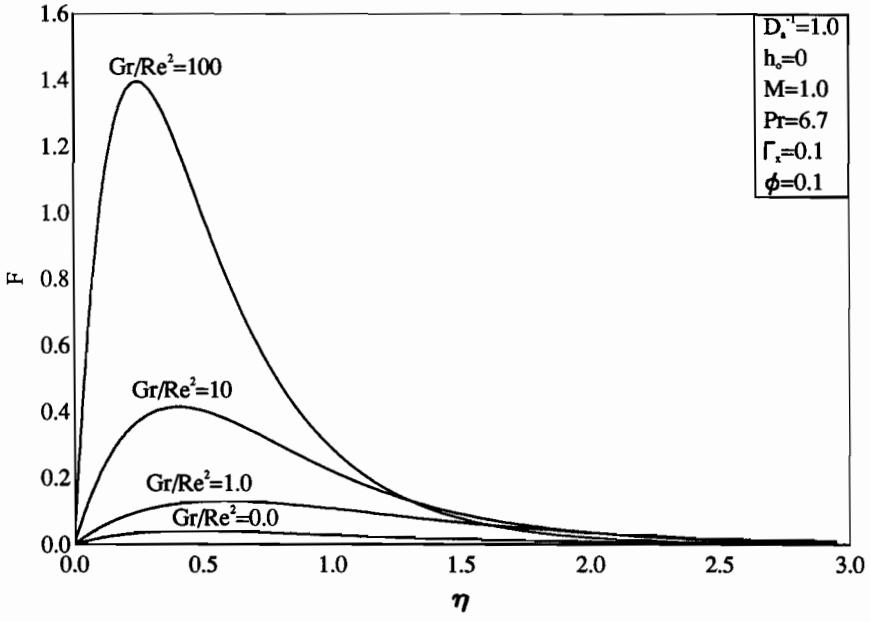

Figure 10. Effects of Gr/Re^2 on tangential velocity profiles.

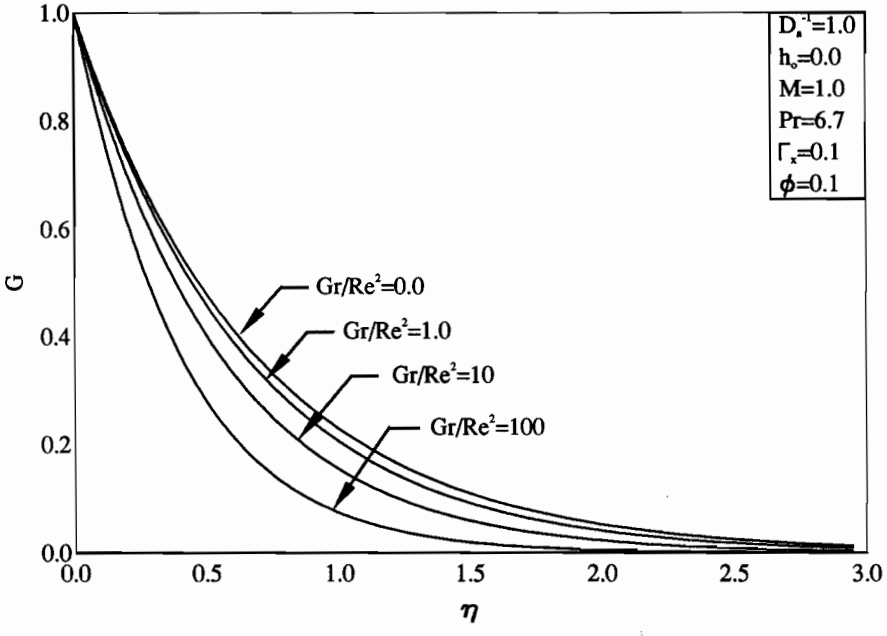

Figure 11. Effects of Gr/Re^2 on circumferential velocity profiles.

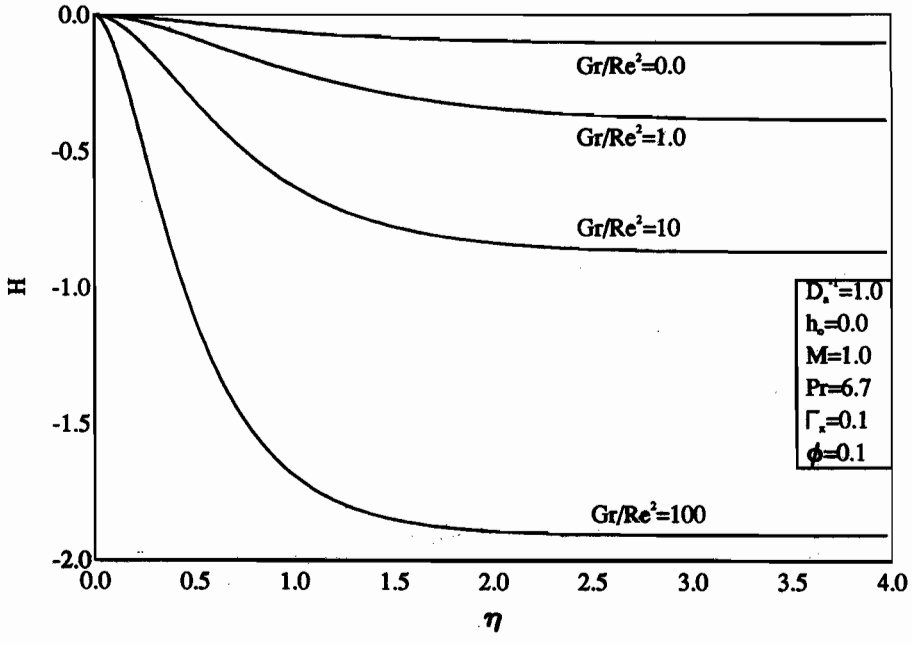

Figure 12. Effects of Gr/Re^2 on normal velocity profiles.

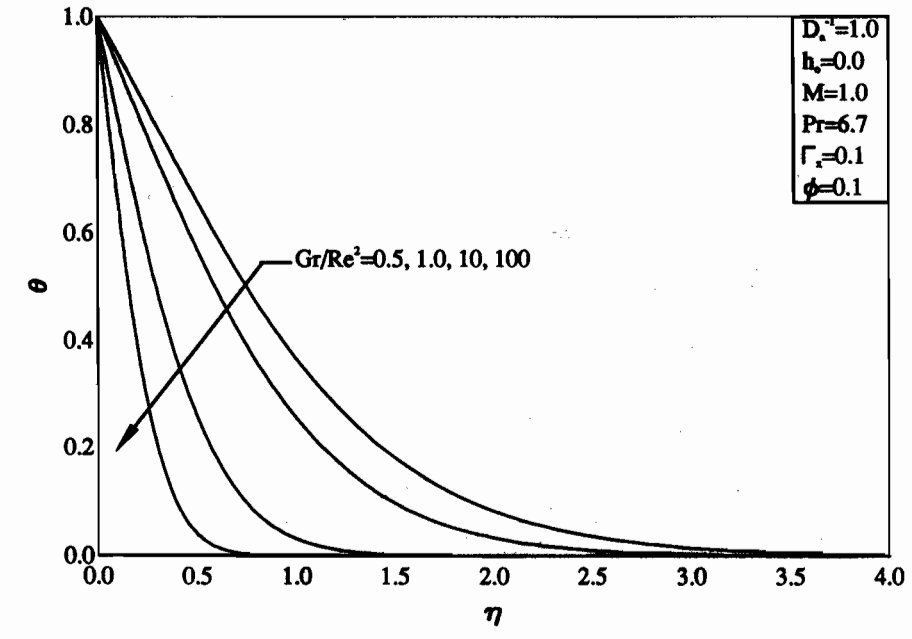

Figure 13. Effects of Gr/Re^2 on temperature profiles.

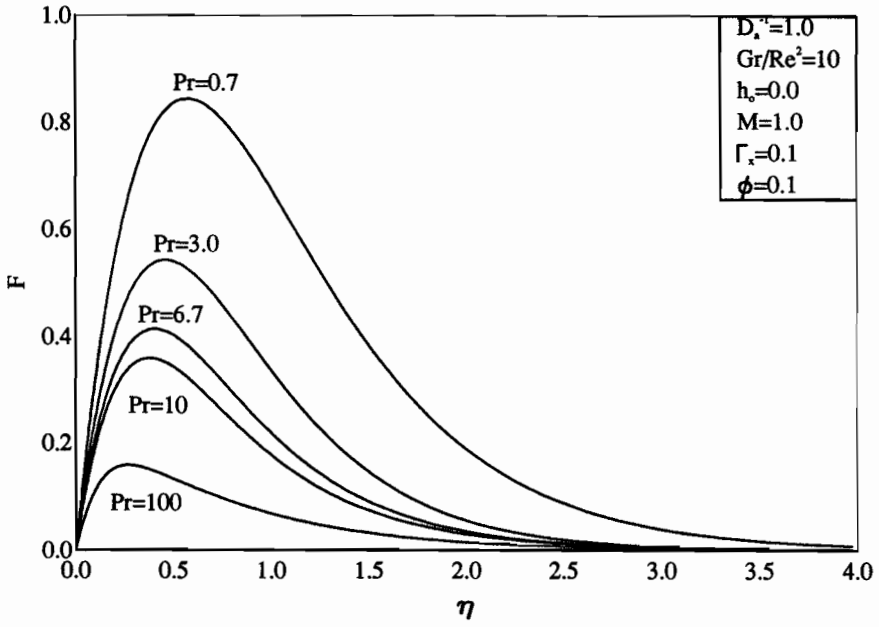

Figure 14. Effects of *Pr* on tangential velocity profiles.

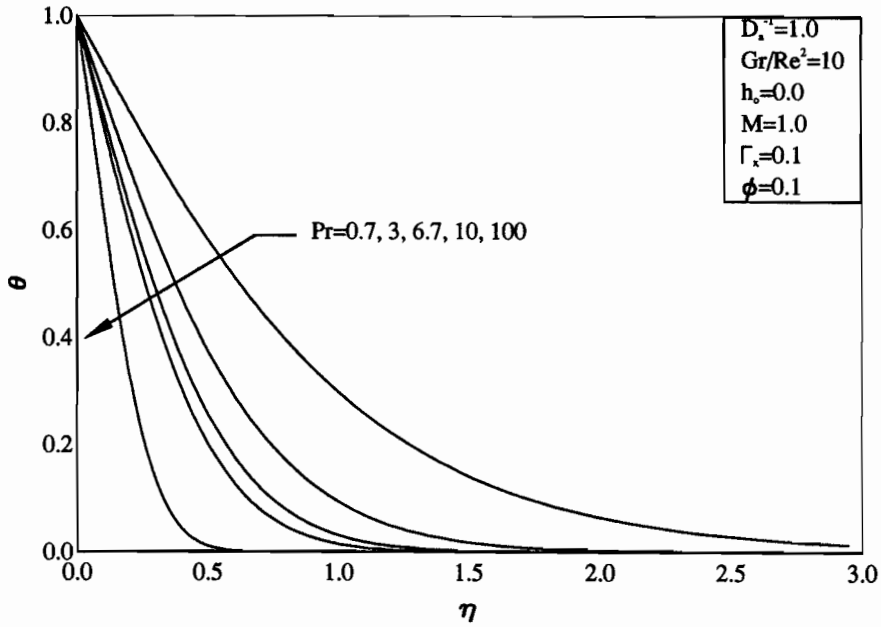

Figure 15. Effects of *Pr* on temperature profiles.

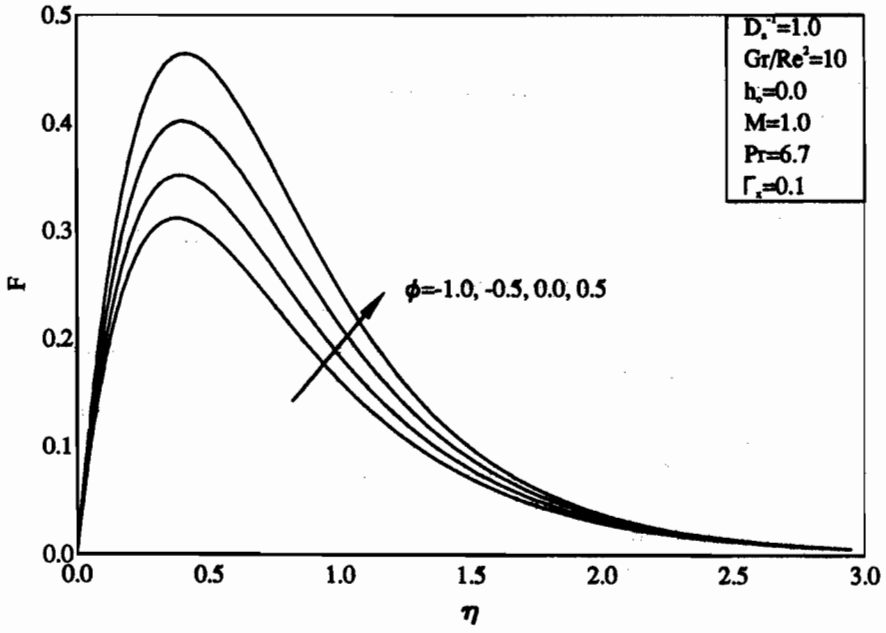

Figure 16. Effects of ϕ on tangential velocity profiles.

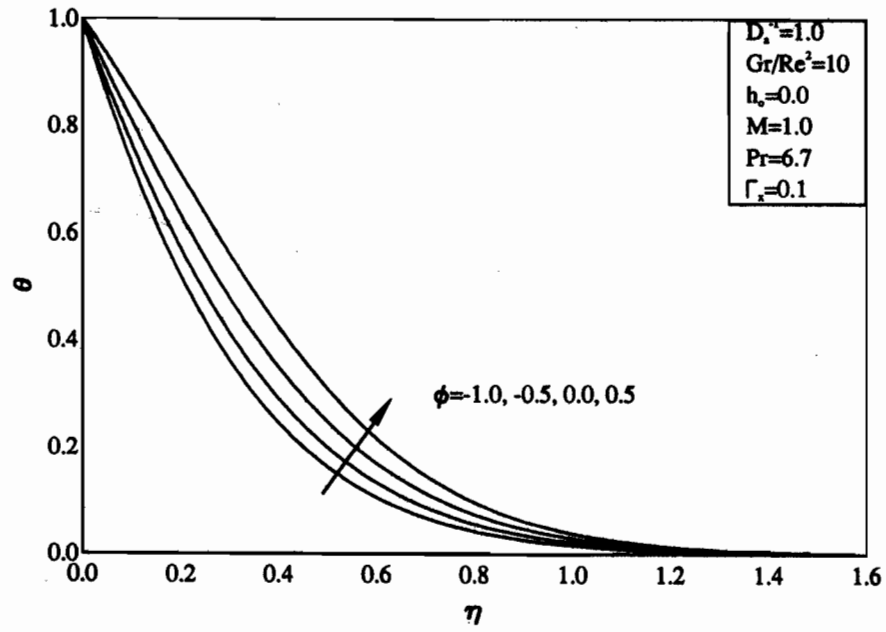

Figure 17. Effects of ϕ on temperature profiles.

Figures 18 and 19 exhibit the variations in the moment coefficient $C_m(=C_M Re^{1/2} \sin \alpha/\pi)$ and the Nusselt number $Nu(=N_q Re^{-1/2})$ as a result of simultaneous changes in the values of the ratio Gr/Re^2, the inverse Darcy number D_a^{-1}, and the dimensionless porous medium inertia coefficient. Γ_x, respectively. It is clearly seen from these figures that while both of C_m and Nu increase with increasing values of Gr/Re^2, the values of C_m increase and the values of Nu decrease as D_a^{-1} increases. In addition, it is observed that increasing Γ_x produces further increases in C_m because, as D_a^{-1}, Γ_x represents resistance to flow while it has no significant changes in Nu.

Figures 20 and 21 depict the effects of Pr and M on C_m and Nu, respectively. The reductions in both the mass flow of ambient fluid near the cone surface and the thermal boundary-layer thickness, mentioned before, as Pr increases cause C_m to decrease and Nu to increase. However, as the strength of the magnetic field represented by the Hartmann number M increases, the values of C_m increase while those of Nu decrease. It is also evident from Fig. 20 that for relatively large values of M, C_m exhibits a linear relation with Pr.

Figures 22 through 25 display the features of C_m and Nu caused by allowing for wall mass transfer ($h_o \neq 0$), increasing buoyancy effects Gr/Re^2, and including the heat generation or absorption effects. It is clear from Figs. 22 and 23 that both C_m and Nu increase if fluid suction is imposed at the cone surface and they decrease if fluid wall blowing exists. Figures 24 and 25 show that as the buoyancy effects Gr/Re^2 increase, both C_m and Nu increase. However, allowing for fluid heat generation increases the values of C_m while it produces reductions in the values of Nu.

CONCLUSION

The problem of steady, laminar, hydromagnetic, boundary-layer, mixed convection flow of an electrically conducting and heat-absorbing or generating fluid induced by a nonisothermal permeable cone embedded in a porous medium rotating at a constant angular speed was investigated numerically. The governing boundary-layer equations were transformed by using similarity variables into ordinary differential equations that were accurately solved by an implicit finite-difference scheme. Comparisons with previously published work on special cases of this problem were performed and found to be in excellent agreement. It was found that the presence of either the magnetic field, heat generation, or the porous medium caused increases in the moment and friction coefficients and reductions in the Nusselt number. However, although imposition of fluid suction at the cone surface caused increases

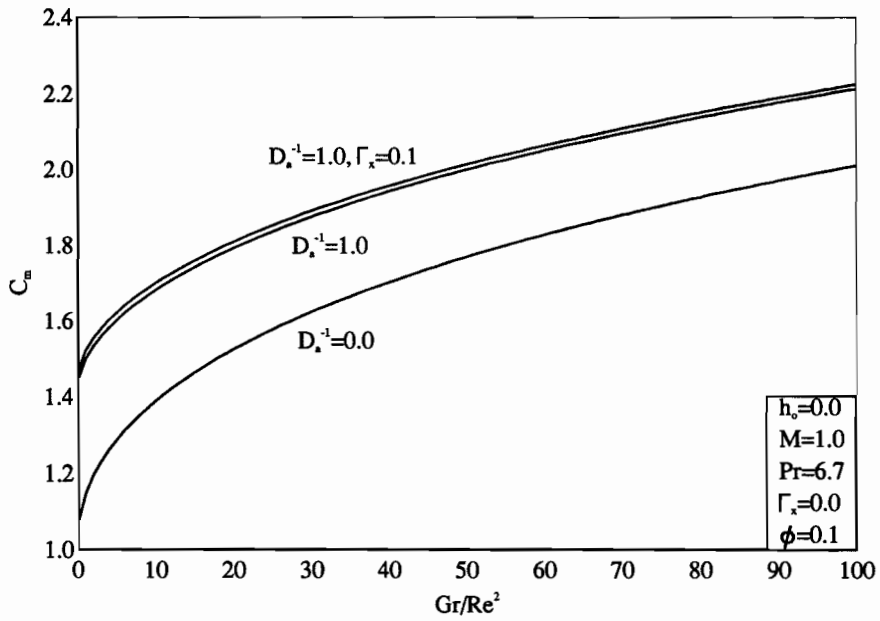

Figure 18. Effects of Gr/Re^2 and D_a^{-1} on moment coefficient.

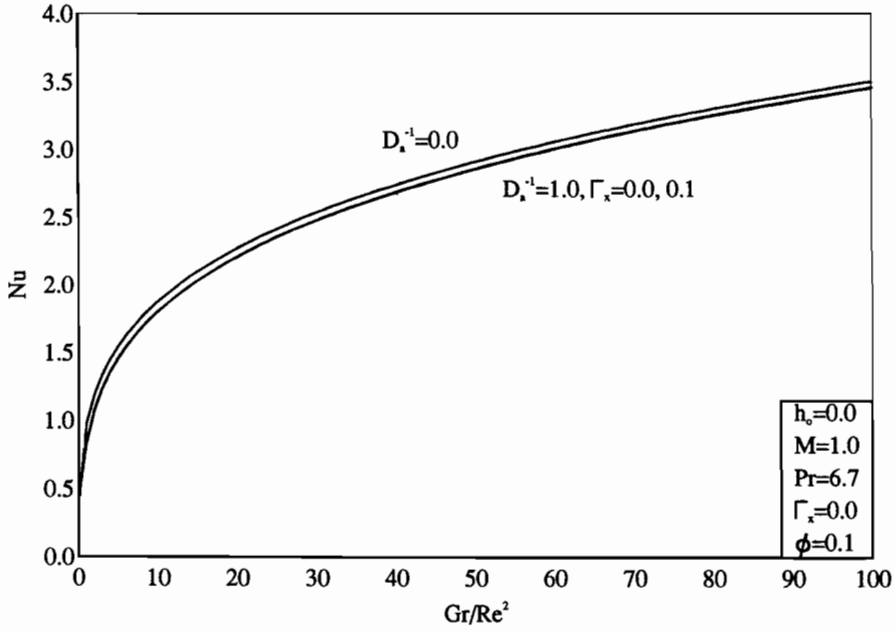

Figure 19. Effects of Gr/Re^2 and D_a^{-1} on Nusselt number.

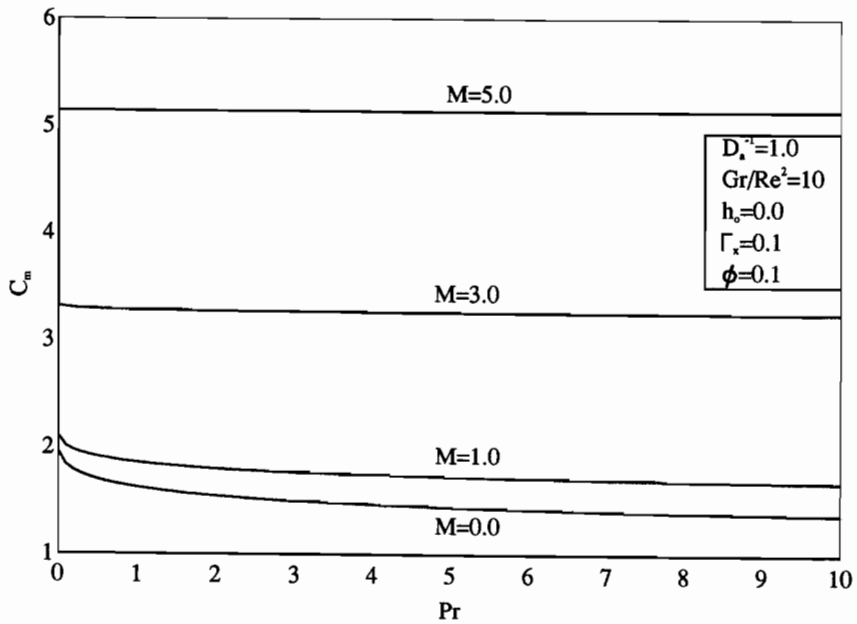

Figure 20. Effects of Pr and M on moment coefficient.

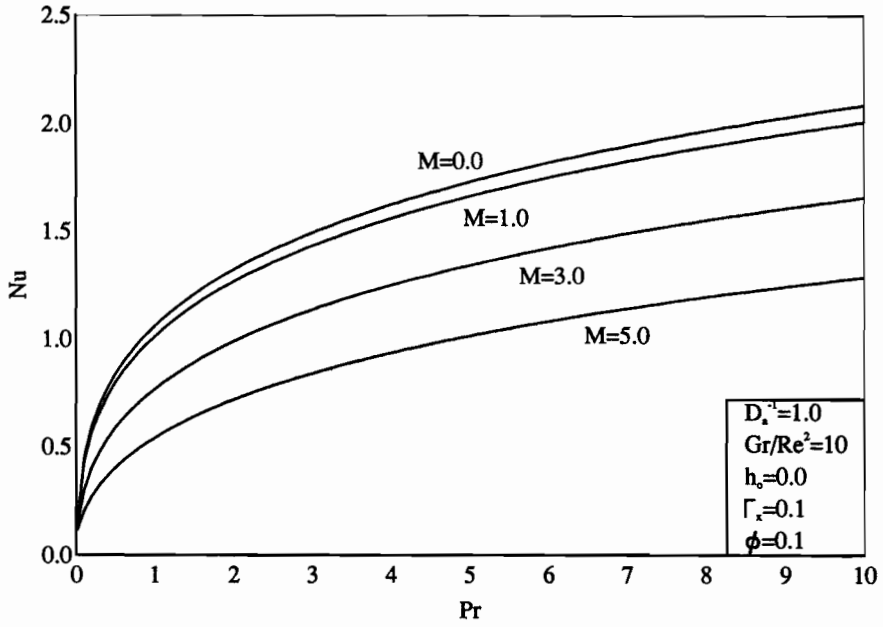

Figure 21. Effects of *Pr* and *M* on Nusselt number.

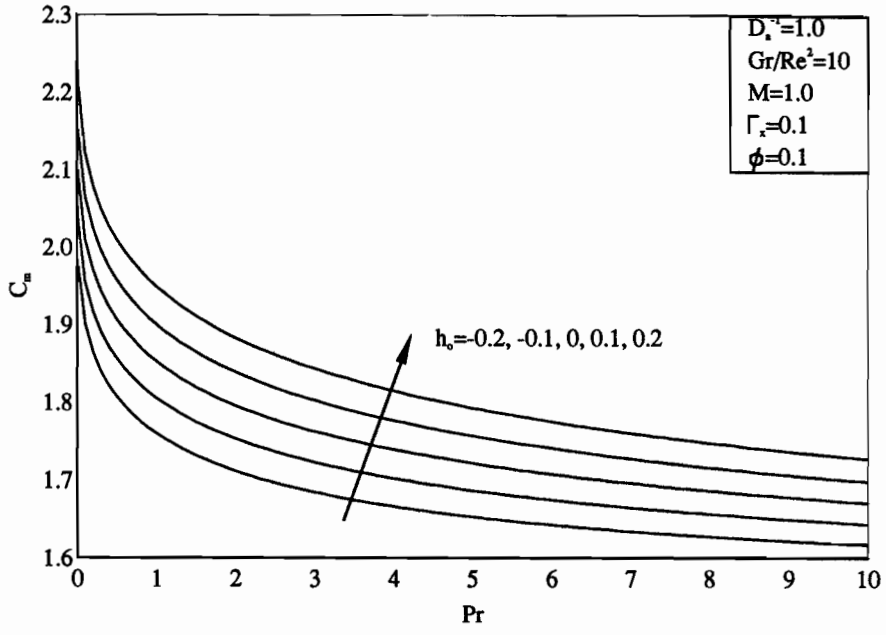

Figure 22. Effects of *Pr* and h_0 on moment coefficient.

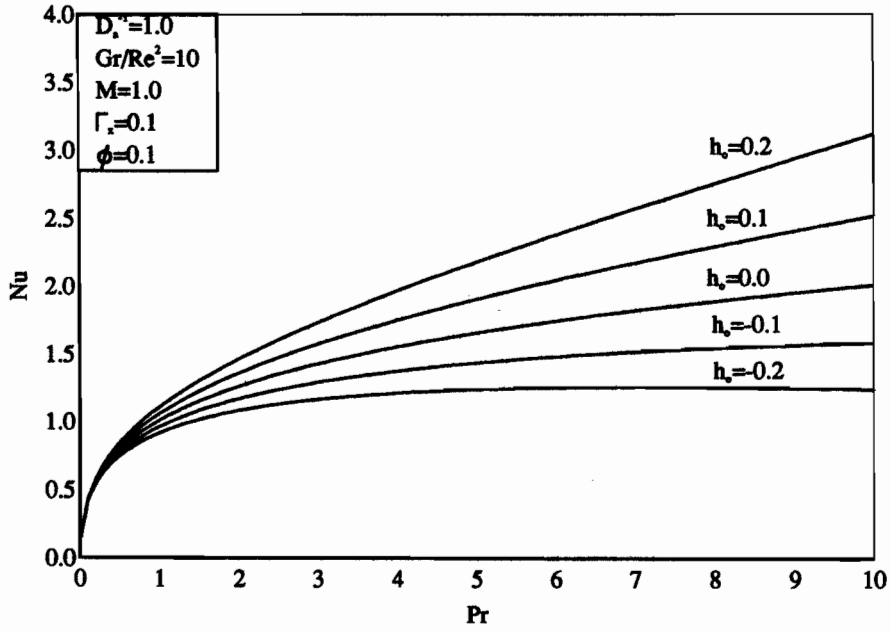

Figure 23. Effects of Pr and h_0 on Nusselt number.

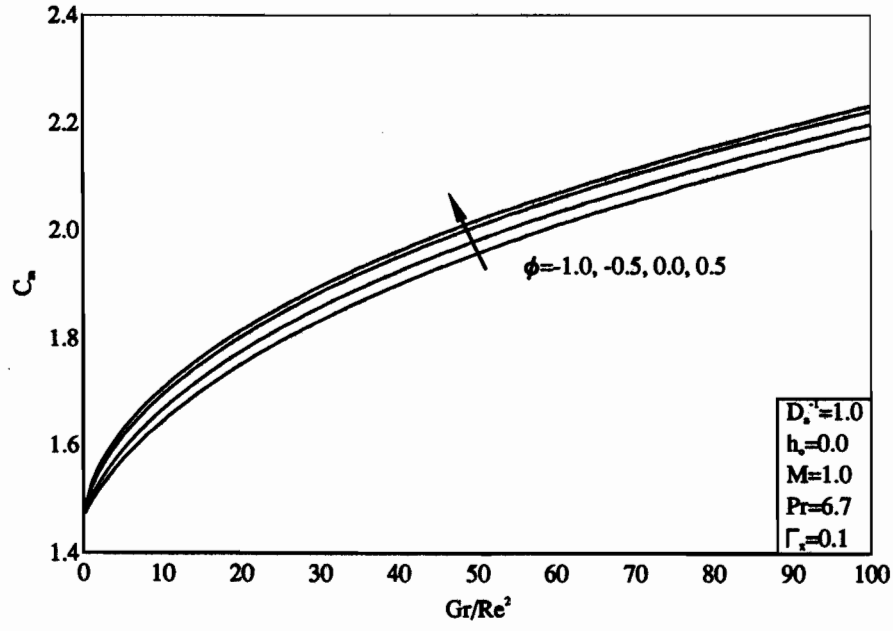

Figure 24. Effects of Gr/Re^2 and ϕ on moment coefficient.

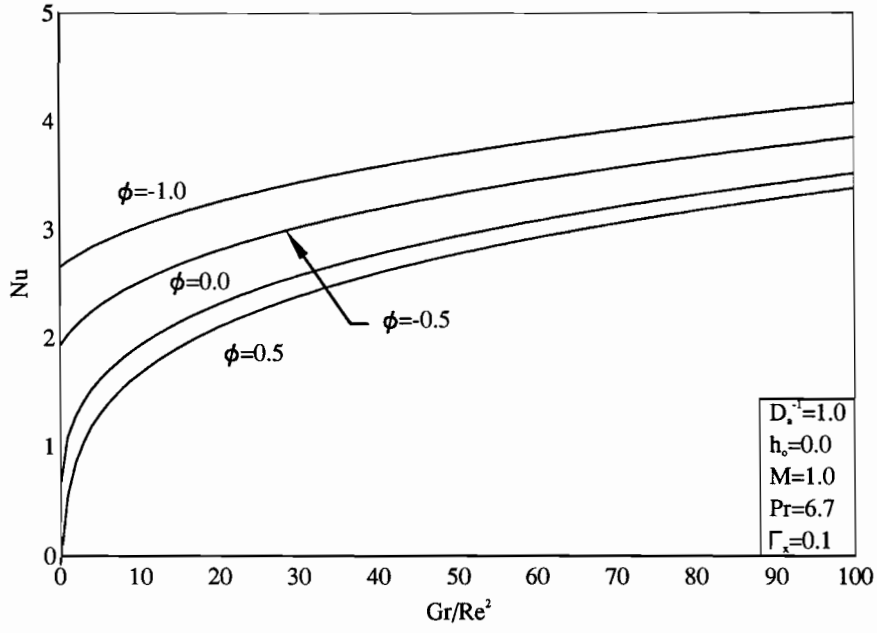

Figure 25. Effects of Gr/Re^2 and ϕ on Nusselt number.

in the moment and friction coefficients, it also produced increases in the wall heat transfer rate represented by the Nusselt number. Furthermore, as reported by previous investigators, increasing either of the fluid Prandtl number or the buoyancy effects caused augmentation in the wall heat transfer. Finally, the moment coefficient was observed to decrease with increasing values of the Prandtl number and to increase with increases in the buoyancy effects. It is hoped that the numerical results presented in this article will be useful for design engineers in designing systems dealing with the flow and heat transfer situation considered in the present work.

REFERENCES

Aldoss, T. K., Al-Nimr, M. A., Jarrah, M. A., and Al-Sha'er, B. J., Magnetohydrodynamic mixed convection from a vertical plate embedded in a porous medium, *Numer. Heat Transfer,* pt. A, vol. 28, pp. 635–645, 1995.

Aldoss, T. K., Chen, T. S., and Armaly, B. F., Mixed convection over nonisothermal horizontal surfaces in a porous medium-the entire regime, *Int. J. Heat Mass Transfer,* vol. 25, pp. 685–701, 1994.

Blottner, F. G., Finite-difference methods of solution of the boundary-layer equations, *AIAA J.,* vol. 8, pp. 193–205, 1970.

Cebeci, T. and Bradshaw, P., *Momentum Transfer in Boundary Layers,* Chaps. 7 and 8, Hemisphere, Washington, D.C., 1977.

Chamkha, A. J., Non-Darcy hydromagnetic free convection from a cone and a wedge in porous media, *Int. Commun. Heat Mass Transfer,* vol. 23, pp. 875–887, 1996.

Chamkha, A. J., Non-Darcy fully developed mixed convection in a porous medium channel with heat generation/absorption and hydromagnetic effects, *Numer. Heat Transfer,* pt A, vol. 32, pp. 635–675, 1997.

Gorla, R. S. R., The effects of uniform suction on the magneto-hydrodynamic flow over a rotating disc, *Int. J. Engng. Fluid Mechan.,* vol. 5, pp. 413–433, 1992.

Hartnett, J. P. and Deland, E. C., The influence of Prandtl number on the heat transfer from rotating non-isothermal disks and cones, *ASME J. Heat Transfer,* vol. 83, pp. 95–96, 1961.

Hering, R. G. and Grosh, R. J., Laminar combined convection from a rotating cone, *ASME J. Heat Transfer,* vol. 85, pp. 29–34, 1963.

Himasekhar, K. and Sarma, P. K., Integral analysis of mixed convective heat transfer from a rotating cone, *Reg. J. Energy Heat Mass Transfer,* vol. 6, pp. 155–160, 1984.

Himasekhar, K. and Sarma, P. K., Effect of suction on heat transfer rates from a rotating cone, *Int. J. Heat Mass Transfer,* vol. 29, pp. 164–167, 1986a.

Himasekhar, K. and Sarma, P. K., Laminar combined convection from a rotating cone to a thermally stratified environment, *ASME J. Heat Transfer,* vol. 108, pp. 973–976, 1986b.

Hossain, M. A., Viscous and Joule heating effect on MHD-free convection with variable plate temperature, *Int. J. Heat Mass Transfer,* vol. 35, pp. 3485–3487, 1992.

Hsieh, J. C., Chen, T. S., and Armaly, B. F., Nonsimilarity solutions for mixed convection from vertical surfaces in a porous medium-variable surface temperature or heat flux, *Int. J. Heat Mass Transfer,* vol. 36, pp. 1485–1493, 1993.

Kafoussias, N. G., MHD free convection flow through a nonhomogeneous porous medium over an isothermal cone surface, *Mech. Res. Commun.,* vol. 19, pp. 89–94, 1992.

Kreith, F., Convective heat transfer in rotating systems, *Adv. Heat Transfer,* vol. 5, pp. 129–251, 1968.

Kumar, S. K., Thacker, W. I., and Watson, L. T., Magnetohydrodynamic flow past a porous rotating disk in a circular magnetic field, *Int. J. Numer. Methods Fluids,* vol. 8, pp. 659–669, 1988.

Kumari, M., Takhar, H. S., and Nath, G., Nonaxisymmetric unsteady motion over a rotating disk in the presence of free convection and magnetic field, *Int. J. Engng. Sci.,* vol. 31, pp. 1659–1668, 1993.

Lai, F. C. and Kulacki, F. A., Non-Darcy mixed convection along a vertical wall in a saturated porous medium, *Int. J. Heat Mass Transfer,* vol. 113, pp. 252–255, 1991.

Lin, H. T. and Lin, L. K., Heat transfer from a rotating cone or disk to fluids of any Prandtl number, *Int. Commun. Heat Mass Transfer,* vol. 14, pp. 323–332, 1987.

Merk, H. J. and Prins, J. A., Thermal convection in laminar boundary layers, I, *Appl. Sci. Res.,* vol. 4, pp. 11–24, 1953.

Minkowycz, W. J., Cheng, P., and Chang, C. H., Mixed convection about a nonisothermal cylinder and sphere in a porous medium, *Numer. Heat Transfer,* vol. 8, pp. 349–359, 1985.

Moalem, D., Steady state heat transfer within porous medium with temperature dependent heat generation, *Int. J. Heat Mass Transfer,* vol. 19, pp. 529–537, 1976.

Nield, D. A., The limitations of the Brinkman–Forchheimer equation in modeling flow in a saturated porous medium and at an interface, *Int. J. Heat Fluid Flow,* vol. 12, pp. 269–272, 1991.

Oehlbeck, D. L. and Erian, F. F., Heat transfer from axisymmetric sources at the surface of a rotating disk, *Int. J. Heat Mass Transfer,* vol. 22, pp. 601–610, 1979.

Raptis, A. A., Flow through a porous medium in the presence of a magnetic field, *Energy Res.,* vol. 10, pp. 97–100, 1986.

Raptis, A. and Kafoussias, N., Heat transfer in flow through a porous medium bounded by an infinite vertical plate under the action of a magnetic field, *Energy Res.,* vol. 6, pp. 241–245, 1982.

Raptis, A. and Singh, A. K., MHD free convection flow past an accelerated vertical plate, *Int. Commun. Heat Mass Transfer,* vol. 10, pp. 313–321, 1983.

Riley, N., Magnetohydrodynamics free convection, *J. Fluid Mech.,* vol. 18, pp. 577–586, 1964.

Sparrow, E. M. and Cess, R. D., Effect of magnetic field on free convection heat transfer, *Int. J. Heat Mass Transfer,* vol. 3, pp. 267–274, 1961.

Takhar, H. S. and Ram, P. C., Magnetohydrodynamics free convection flow of water at 40° through a porous medium, *Int. Commun. Heat Mass Transfer,* vol. 21, pp. 371–376, 1994.

Takhar, H. S., Surma Devi, C. D., and Nath, G., Unsteady laminar incompressible boundary layer flows over a rotating disk with an applied magnetic field, *Ind. J. Technol.,* vol. 25, pp. 155–159, 1987.

Tien, C. L., Heat transfer by laminar flow from a rotating cone, *ASME J. Heat Transfer,* vol. 82, pp. 252–253, 1960.

Vafai, K. and Tien, C. L., Boundary and inertia effects on flow and heat transfer in porous media, *Int. J. Heat Mass Transfer,* vol. 24, pp. 195–203, 1981.

Vajravelu, K. and Nayfeh, J., Hydromagnetic convection at a cone and a wedge, *Int. Commun. Heat Mass Transfer,* vol. 19, pp. 701–710, 1992.

Wang, T. Y. and Kleinstreuer, C., Similarity solutions of combined convection heat transfer from a rotating cone or disk to non-Newtonian fluids, *J. Heat Transfer,* vol. 112, pp. 939–944, 1990.

Wang, T. Y., Kleinstreuer, C., and Chiang, H., Mixed convection from a rotating cone with variable surface temperature, *Numer. Heat Transfer,* pt A, vol. 25, pp. 75–83, 1994.